Homogenization expansion for resonances of microstructured photonic waveguides

Steven E. Golowich and Michael I. Weinstein

Mathematical Sciences Research, Bell Laboratories, Lucent Technologies, Murray Hill, New Jersey 07974

Received August 27, 2002; revised manuscript received October 28, 2002

We develop a homogenization expansion approach to photonic waveguides whose transverse structures are N-fold rotationally symmetric. Examples include microstructured or holey optical fibers with air holes arranged in one or more concentric rings. We carry out a homogenization expansion for large N about the $N = \infty$ limit. Our multiple scale analysis applies to the scalar approximation of structures in which the microfeatures have arbitrary geometry and large index contrasts and lead to a natural efficient computational algorithm for the waveguide modes and spectral characteristics. In this paper we focus on structures that possess leaky modes. The leading order ($N = \infty$) equations describe the modes of an averaged structure. We derive an expansion in powers of $1/N$ of corrections to the leading order behavior and show that the leading order nontrivial contribution arises at order $1/N^2$. We numerically calculate this leading order correction to the complex effective indices (scattering resonances) for the leaky modes of various microstructured photonic waveguides whose imaginary parts give the leakage rates. We observe that in many instances a two-term truncation of the homogenization expansion gives good agreement with full simulations, even for fairly small values of N, whereas the leading order (averaged) theory yields a substantial underestimate of the leakage rates.

OCIS codes: 000.3860, 060.2280, 060.2400.

1. INTRODUCTION

There is currently a great deal of interest in the propagation of light in microstructured or holey optical fiber waveguides with novel cross sections that consist of holes surrounded by glass. The holes can be empty or filled with a material chosen to influence the propagation. The ability to vary the transverse geometry because of advances in fabrication technology, combined with the large index contrasts possible with such structures, give multiple new degrees of freedom that potentially enable designs with radically different properties than are possible with standard fiber.

Numerous interesting phenomena have already been observed in such waveguides. Among them are (i) guidance by the interference-based photonic bandgap effect in fibers with an air core and (truncated) transverse periodic lattice of air holes,[1] (ii) variability of chromatic dispersion with a microstructure,[2,3] and (iii) resulting nonlinear effects in newly accessible spectral ranges that are due to microstructure-induced shifting of the zero dispersion point in glass core fiber.[2]

Efficient and accurate mathematical modeling of light propagation in microstructured fiber is clearly necessary for their design and analysis. A feature of most such structures is that they are inherently leaky because of the existence of paths that lead from the core to the cladding that avoid the holes and pass through only the background glass. Such structures support no true guided modes, but they will have leaky modes characterized by complex-valued propagation constants or effective indices (scattering resonances); the leakage rate is given by the imaginary part. Physically, this leakage is due to a combination of tunneling through the holes and propagating through the glass that surrounds them. The ability to calculate such rates is clearly of fundamental importance. Other quantities of interest include the real parts of the effective indices, which determine the response of the structure to longitudinal variations such as gratings, and the dispersion relations of the various leaky modes, which might be quite unusual compared with standard waveguides, due to the presence of large index contrasts and interference effects.

There have been many numerical studies of microstructure fiber based on direct numerical calculation of static Maxwell's equations to determine the system's modes; some are also able to capture the attenuation rates. A variety of methods have been used, among them multipole expansion,[4] which works well for structures with circular holes; more general expansions in local bases[5] and Fourier decompositions,[6] which are applicable to more general geometries; and scalar and vector beam propagation,[4,7] which are applicable to general geometries but have limitations in computing small attenuation rates and have proved problematic in some geometries.[8] All these techniques have the characteristic that the computational difficulty of the calculations increase with the complexity of the structures. By contrast, it has been shown[9] that, for a fine enough microstructure, an angularly averaged index profile gives accurate values for the real part of the effective indices of the leaky modes; the leakage rates, however, are often greatly underestimated.

We consider the waveguide problem in the scalar approximation. We develop a multiple scale perturbation theory of a large class of sufficiently oscillatory structures, suitable for the analytical study and efficient nu-

merical computation of such quantities as leakage rates, group velocities, and dispersion, that becomes more accurate as the transverse structure becomes more oscillatory, in a sense that we make precise below. If the transverse structure is invariant under rotation by $2\pi/N$ (e.g., in the case of a single ring of N holes uniformly distributed in an annulus), we expand the leaky modes and the effective indices (scattering resonances) in powers of $1/N$. The leading order in our expansion turns out to be the averaged or homogenized index profile[10,11] referred to above. In this paper we focus primarily on the derivation and computation of the leading order corrections (order N^{-2}), caused by the microstructure, of both the real and the imaginary parts of the effective indices of the leaky modes of such averaged profiles. Since the leading order behavior is given by a homogenized (in angle) effective medium, we refer to this expansion as a homogenization expansion. Results of first-order corrections to homogenized eigenvalues of periodic composite media have been obtained within a different context.[12,13]

A few of the consequences of the homogenization expansion and numerical implementation that we wish to highlight are listed in the following subsections.

A. Computational Algorithm

Our analytic theory leads to a natural efficient computational algorithm for the modes and spectral characteristics, e.g., leakage rates, dispersion. Multiscale analysis enables us to eliminate the stiff aspects of the computation that are due to the rapidly varying structure. Therefore, one can expect significant reduction in computational effort. This is especially important for increasingly microstructured media, for which the approximation improves, as well as for simulation-based optimization of light-guiding characteristics.

B. Arbitrary Geometry and Index Contrasts

Although we require N-fold symmetry of the structure, the individual microfeatures can have arbitrary geometry and large index contrasts. In our current implementation, we approximate an arbitrary microfeature by a simple layered structure, defined in subsection 7.B, for which many of the calculations required can be done explicitly.

C. Good Agreement with Full Numerical Simulation

In Section 5 we present results of numerical simulations based on our theory for several waveguides with transverse microstructure. We focus on the complex effective indices as they vary with the geometry of the microstructure. We are particularly interested in the imaginary parts of the effective indices that correspond to the leakage rates. We present comparisons of our predicted loss rates with the results that were obtained when the Helmholtz equation was solved directly by the Fourier decomposition algorithm[6] and the vector Maxwell's equations by multipole methods.[4] One expects the homogenization theory to be valid when the wavelength of light is long compared with the individual microfeatures. We found good agreement of our theory with full simulations even in regimes where λ_{fs}/d, the ratio of wavelength to length scale of microfeatures, is as small as 3/2. Although the expansion is derived for N large, with the $N = \infty$ limit being the leading order term, examples in Section 5 show agreement in cases for which $N = 3$ and $N = 6$. We also observe the expected departure of our approximate methods from the results of full simulations for sufficiently small λ_{fs}/d.

D. Sensitivity of Leakage Rates to Microstructure

In Section 5 we used our theory to compute the first two nontrivial terms of the effective indices (scattering resonances) of the leaky modes. The first term corresponds to an average theory and the second term is a correction that is due to microstructure. The imaginary parts of the effective indices, corresponding to the leakage rates, are sensitive to the introduction of microstructure and their accurate approximation requires both terms. In contrast, as noted above, the real parts of the effective indices are relatively insensitive to microstructure and are well captured by the leading order term.

E. Corrected Fields

We find that corrections that are due to microstructure of the mode fields predicted by the averaged structure are compactly supported in space if the microstructure perturbation is compactly supported in space. This is not possible for the true solution of the mathematical model. An additional observation indicating a limitation of the homogenization expansion is seen for a family of structures that consist of two rings of holes, parameterized by the relative phase angle of the arrangement in one ring to another. Since the variation in refractive index in one ring occurs on a disjoint set from that for the second ring, we find the homogenization expansion predicts complex effective indices that are independent of the phase angle. This suggests that in the regime in which certain interference effects are important, the asymptotic expansion of this paper could have limited use. Nevertheless, we have proved[14] that two-term approximate expansion of modes and effective indices is valid for sufficiently large N. This rigorous theory gives field corrections that at any finite N are not compactly supported.

Mathematically, the leaky modes and effective indices are obtainable from the solution of the eigenvalue problem for the Schrödinger equation

$$[-\Delta_\perp + V(r,\ \theta,\ N\theta)]\psi = E\psi,$$
$$\psi \ \text{outgoing as} \ r = |\mathbf{x}| \to \infty; \tag{1.1}$$

we formulate this as a scattering resonance problem in Section 3. Here, $\Delta_\perp$ denotes the two-dimensional Laplace operator in the transverse plane. (When the context is clear, we shall omit the subscript $\perp$.) Since the outgoing radiation condition at infinity is not self-adjoint, we expect eigenvalues E to be complex. The attenuation or leakage rates are given by the imaginary part of

$$\beta = (k^2 n_g{}^2 - E)^{1/2}, \tag{1.2}$$

where n_g denotes a background refractive index. Of importance in optics is the effective index

$$n_{\mathrm{eff}} \equiv \beta/k, \tag{1.3}$$

where $k = 2\pi/\lambda_{fs}$ and λ_{fs} is the free-space wavelength. The effective index is a complex quantity for leaky waveguides. In Section 5 the real and imaginary parts of β, $\Re\beta$, and $\Im\beta$ are displayed in plots of

$$\gamma \equiv 10 \log_{10} \frac{\text{power input}}{\text{power output}} \sim \Im\beta$$

versus $\Re n_{\text{eff}} = k^{-1} \Re\beta$. We give attenuation rates γ in units of dB/cm, whereas $\Re n_{\text{eff}}$ is dimensionless.

In Section 6 we numerically investigate the convergence of our expansion for increasing N. To conclude the paper, in Section 8 we give a brief summary. We also relate the current work to a forthcoming paper[14] that contains a rigorous perturbation theory of a general class of scattering resonance problems with rapidly varying and high contrast potentials. In particular, the latter study implies the validity of our homogenization expansion and error estimates for the two-term truncation we use in our simulations.

2. MAXWELL'S EQUATIONS IN A WAVEGUIDE

Consider a waveguide with refractive-index profile $n(x)$. If the medium is nonmagnetic and there are no sources of free charge or current, then the time-harmonic Maxwell equations imply that the transverse components of the electric field $\mathbf{E}_\perp$, $\mathbf{E}_\perp \exp(i\beta x_3)\mathbf{e}_\perp$, obey[15]

$$[\Delta_\perp + k^2 n^2(\mathbf{x}_\perp) - \beta^2]\mathbf{e}_\perp = \mathscr{T}_1 \ \mathbf{e}_\perp, \tag{2.1}$$

where

$$\mathscr{T}_1 \ \mathbf{e}_\perp \equiv -\boldsymbol{\nabla}_\perp(\mathbf{e}_\perp \cdot \boldsymbol{\nabla}_\perp \ln n^2).$$

We work in the scalar approximation, which entails neglecting the term $\mathscr{T}_1 \ \mathbf{e}_\perp$ in Eq. (2.1) that arises because of the vector nature of the fields. For modes that are localized away from the microstructure, which includes most of the examples in Section 5, the vector corrections are expected to be small because the field $\mathbf{e}_\perp$ is small at the interfaces, which are the only places at which it contributes. However, this will not be true in other examples of interest, and we expect that our methods can be extended to the full vector case. In any case, we do not discuss vector effects further in this work.

In the scalar approximation the components of $\mathbf{e}_\perp$ satisfy independent scalar Helmholtz equations. We let φ denote either of these transverse components. Then,

$$(\Delta_\perp + k^2 n^2)\varphi = \beta^2 \varphi, \tag{2.2}$$

where $\Delta_\perp$ denotes the Laplace operator in the transverse variables $x_\perp = (x_1, x_2)$.

Introducing the notation

$$V = k^2({n_g}^2 - n^2), \quad E = k^2 {n_g}^2 - \beta^2, \tag{2.3}$$

the equation for φ and the propagation constant β can be viewed as a Schrödinger equation with potential $V(\mathbf{x}_\perp)$ and energy parameter E:

$$\mathcal{L}\varphi \equiv (-\Delta_\perp + V)\varphi = E\varphi. \tag{2.4}$$

Corresponding to the physical problem described in Section 3 for some $r_* > 0$, we assume that

$$V(\mathbf{x}) \geqslant 0, \quad \text{for all } \mathbf{x},$$

$$V(\mathbf{x}) \equiv 0, \quad \text{for } |\mathbf{x}| \geqslant r_*. \tag{2.5}$$

The potential V therefore does not support bound states (guided modes) and has only scattering states (radiation modes) along with scattering resonances (leaky modes).

3. RESONANCE PROBLEM FOR MICROSTRUCTURE WAVEGUIDES

To fix ideas, consider a cylindrical waveguide composed of two materials g and h, with corresponding refractive indices n_g and n_h. We specify a transverse cross section of the waveguide in the two-dimensional plane, with coordinates $\mathbf{x} = (x_1, x_2) = (r, \theta)$. In Fig. 1 we show a schematic picture of a glass waveguide with a single ring of 12 air holes in a solid glass cylinder. Four regions are illustrated: A_1, the region $|\mathbf{x}| \leqslant R_{\text{in}}$, a disk of glass with refractive index n_g; A_2, the region $R_{\text{in}} \leqslant |\mathbf{x}| \leqslant R_{\text{out}}$, an annular region with 12 equally spaced air holes; A_3, the region $R_{\text{out}} \leqslant |\mathbf{x}| \leqslant R_{\text{clad}}$ that consists of a solid glass $n = n_g$, and finally, A_4, the region $|\mathbf{x}| \geqslant R_{\text{clad}}$ that consists of air $n = n_h$.

We are interested in how well light is confined to the core (A_1) region in such a microstructure fiber. This structure has actual guided in addition to leaky modes that are due to the lower refractive index of region A_4. However, we view any propagation of light from A_1 to A_3 as loss. Therefore, the appropriate mathematical problem for our purposes is the mode equation (2.4) posed on the spatial domain $\{|\mathbf{x}| \leqslant R_{\text{in}}\} \cup \{R_{\text{in}} \leqslant |\mathbf{x}| \leqslant R_{\text{out}}\} \cup \{R_{\text{out}} \leqslant |\mathbf{x}|\}$ subject to an outward-going radiation condition as $|\mathbf{x}| \to \infty$. In practice, the glass optical fiber is usually coated with a high-index and a high-loss polymer, so any light that does leak into A_3 is rapidly attenuated, which provides further justification for the use of this boundary condition.

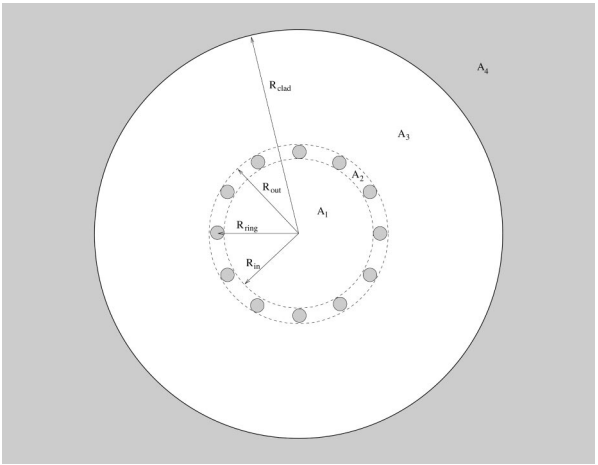

Fig. 1. Cross section of a microstructured waveguide.

We now present a more general mathematical formulation of this *scattering resonance problem*. Given a potential (index profile) $V = V(r, \theta)$ of compact support, we seek E and nonzero φ for which

$$\mathcal{L}\varphi \equiv (-\Delta + V)\varphi = E\varphi \tag{3.1}$$

subject to the outward-going radiation condition, as $r \to \infty$. We call a pair (φ, E) a scattering resonance pair, which is also sometimes called a quasi-resonance.[16]

In our setting, the radiation condition can be simply described. Because $V(r)$ is identically zero for $r \geqslant r_*$, Eq. (2.4) becomes

$$-(\Delta_\perp + E)\varphi = 0, \quad r \geqslant r_*. \tag{3.2}$$

Solutions of Eq. (3.2) can be expanded in a series:

$$\varphi = \sum_{l=-\infty}^{+\infty} [c_l^{(1)} \exp(il\theta) H_l^{(1)}(\sqrt{E}r) + c_l^{(2)} \exp(il\theta) H_l^{(2)}(\sqrt{E}r)], \tag{3.3}$$

where $H_l^{(1)}$ and $H_l^{(2)}$ are first and second Hankel functions of order l.[17] Therefore the requirement that φ be outgoing is equivalent to the vanishing of all coefficients $c_l^{(2)}$ in Eq. (3.3):

$$\text{outward going radiation} \Leftrightarrow c_l^{(2)} = 0 \text{ for all } l. \tag{3.4}$$

Since Eq. (3.4) is a non-self-adjoint boundary condition at infinity, E can be expected to be complex. However, there are constraints on the location of E in the complex plane. For the φ to be oscillatory at infinity, we must have $\Re E > 0$, and for φ to be outgoing $\Re\sqrt{E} > 0$. Furthermore, $\Im E \leqslant 0$. If $\Im E > 0$, then $\Im\sqrt{E} > 0$. From the series expansion in Eq. (3.3) with $c_l^{(2)} = 0$ we conclude that φ exponentially decays as $r \to \infty$ and is therefore an eigenstate of the self-adjoint operator $\mathcal{L}$ with a nonreal eigenvalue. This yields a contradiction. To summarize:

If E is an energy for which there is a solution of the resonance problem, then $\Re E > 0$ and $\Im E \leqslant 0$. Correspondingly, from Eq. (2.3) we have $\Re\beta > 0$ and $\Im\beta > 0$. Since $\mathbf{E}_\perp(\mathbf{x}) = \mathbf{e}_\perp(\mathbf{x}_\perp)\exp(i\beta x_3)$, the complex resonances E correspond to the radiative decay or leakage rates of the structure.

4. MULTIPLE SCALES AND HOMOGENIZATION EXPANSION

In this section we derive a multiple scale expansion of solutions to the resonance problem for microstructures, giving a homogenized (averaged) theory at leading order plus systematically computable corrections. We carry out the analysis for a class of potentials V with the dependence of

$$V = V(r, \theta, N\theta) = V(r, \theta, \Theta), \tag{4.1}$$

where V is 2π periodic in θ and Θ. Thus Eq. (4.1) allows both a slow and a fast angular modulation of the index profile. In the special case where V does not depend on θ and we have $V = V(r, N\theta)$, the potential corresponds to an index profile with an N-fold symmetry. Assume that $V \geqslant 0$ and that for some r_*, $V(r) \equiv 0$ for $r \geqslant r_*$. We show the following.

Theorem: Homogenization Expansion
The resonance mode problem [see Eqs. (3.1)–(3.4)] has, for large N, solutions with the formal expansion

$$\varphi(r, \theta; N) = \Phi^{(N)}(r, \theta, \Theta), \quad \Theta = N\theta$$

given by

$$\Phi^{(N)} = \Phi_0 + \frac{1}{N^2}\Phi_2 + \mathcal{O}\left(\frac{1}{N^3}\right),$$

$$E^{(N)} = E_0 + \frac{1}{N^2}E_2 + \mathcal{O}\left(\frac{1}{N^3}\right). \tag{4.2}$$

Thus, corrections that are due to a microstructure begin at $\mathcal{O}(N^{-2})$.

- $[\Phi_0(r, \theta), E_0]$ is a nontrivial solution of the resonance problem:

$$\mathcal{L}_{\text{av}}\Phi_0 = E_0\Phi_0, \tag{4.3}$$

where Φ_0 is subject to the outward-going radiation condition in Eq. (3.4), and the averaged operator is given by

$$\mathcal{L}_{\text{av}} \equiv \frac{1}{2\pi}\int_0^{2\pi} \mathcal{L}\, d\Theta \equiv -\Delta_\perp + V_{\text{av}}(r, \theta). \tag{4.4}$$

- $\Phi_2 = \Phi_2^{(p)} + \Phi_2^{(h)}$, where $\Phi_2^{(p)}$ is the mean zero solution [easily derived from the Fourier series of $V(\cdot, \cdot, \Theta)$] of

$$\frac{1}{r^2}\partial_\Theta{}^2\Phi_2^{(p)} = [V(r, \theta, \Theta) - V_{\text{av}}(r, \theta)]\Phi_0(r, \theta) \tag{4.5}$$

and $[\Phi_2^{(h)}, E_2]$ solves

$$(\mathcal{L}_{\text{av}} - E_0)\Phi_2^{(h)} = \left\{E_2 + \frac{r^2}{2\pi}\int_0^{2\pi} |\partial_\Theta{}^{-1}[V(r, \theta, \Theta) - V_{\text{av}}(r, \theta)]|^2 d\Theta\right\} \times \Phi_0(r, \theta). \tag{4.6}$$

Finally, E_2 is uniquely determined by the condition that Eq. (4.6) has a solution that satisfies an outgoing radiation condition at $r = \infty$; see Eq. (3.4).

- This yields an approximate solution of the scalar wave equation and an approximation (neglecting vector effects) of the transverse electric field $\mathbf{E}_\perp$ of Maxwell's equations:

$$\mathbf{E}_{\perp,q}(\mathbf{x}; \beta) \sim \exp[i(\beta x_3 - \omega t)]\left[\Phi_0(|\mathbf{x}_\perp|, \theta; \omega) + \frac{1}{N^2}\Phi_2(|\mathbf{x}_\perp|, \theta, N\theta; \omega) + \mathcal{O}\left(\frac{1}{N^3}\right)\right].$$

Here, $q = 0$ or 1, $\omega = ck$, and $\beta = (k^2 n_g{}^2 - E)^{1/2} = \Re\beta + i\Im\beta$, with $\Im\beta > 0$. $\mathbf{E}_{\perp,q}(\mathbf{x}_\perp, x_3)$ decays with increasing x_3 and is therefore a leaky mode. These modes are not square integrable.

In Section 5 we present the results of numerical simulations performed by using a two-term truncation of our homogenization expansion, compare them with published computations of solutions to the full problem, and discuss the question of convergence of our expansion.

A. Multiple Scale Expansion

Because of the rapidly varying coefficient in Eq. (2.4) we expect rapid variations in its solutions. We therefore explicitly introduce the fast angular variable

$$\Theta = N\theta \tag{4.7}$$

and view φ as a function of the three independent variables r, θ, and Θ:

$$\varphi(r,\ \theta) = \Phi(r,\ \theta,\ \Theta). \tag{4.8}$$

Here, we use polar coordinates $x = (r,\ \theta)$ and note that

$$\Delta_\perp = \Delta_r + \frac{1}{r^2}\partial_\theta{}^2, \tag{4.9}$$

where Δ_r denotes the radial part of the transverse Laplacian:

$$\Delta_r \equiv \partial_r{}^2 + \frac{1}{r}\partial_r .$$

Thus, the operator ∂_θ is replaced by $\partial_\theta + N\partial_\Theta$ and Eq. (2.4) becomes

$$\left[-\Delta_r - \frac{1}{r^2}(\partial_\theta + N\partial_\Theta)^2 + V(r,\ \theta,\ \Theta)\right]\Phi = E\Phi, \tag{4.10}$$

Equivalently,

$$\left(\mathcal{L} - \frac{2N}{r^2}\partial_\theta\partial_\Theta - \frac{N^2}{r^2}\partial_\Theta{}^2\right)\Phi = E\Phi. \tag{4.11}$$

We seek an expansion of Φ and E in the small parameter $1/N$:

$$\Phi^{(N)} = \Phi_0 + \frac{1}{N}\Phi_1 + \frac{1}{N^2}\Phi_2 + \frac{1}{N^3}\Phi_3 + \frac{1}{N^4}\Phi_4 + \Phi_5{}^{(N)},$$

$$E^{(N)} = E_0 + \frac{1}{N}E_1 + \frac{1}{N^2}E_2 + E_3{}^{(N)}. \tag{4.12}$$

Here, $\Phi_j = \Phi_j(r,\ \theta,\ \Theta)$.

Substitution of Eqs. (4.12) into Eq. (4.11) and equating like powers of $1/N$ we obtain a hierarchy of equations that arise at each order in $1/N$. We display the first five equations of this hierarchy:

$$\mathcal{O}(N^2): \quad \frac{1}{r^2}\partial_\Theta{}^2\Phi_0 = 0, \tag{4.13}$$

$$\mathcal{O}(N): \quad \frac{1}{r^2}\partial_\Theta{}^2\Phi_1 = -\frac{2}{r^2}\partial_\theta\partial_\Theta\Phi_0, \tag{4.14}$$

$$\mathcal{O}(1): \quad \frac{1}{r^2}\partial_\Theta{}^2\Phi_2 = -\frac{2}{r^2}\partial_\theta\partial_\Theta\Phi_1 + (\mathcal{L} - E_0)\Phi_0, \tag{4.15}$$

$$\mathcal{O}(N^{-1}): \quad \frac{1}{r^2}\partial_\Theta{}^2\Phi_3 = -\frac{2}{r^2}\partial_\theta\partial_\Theta\Phi_2 + (\mathcal{L} - E_0)\Phi_1 - E_1\Phi_0, \tag{4.16}$$

$$\mathcal{O}(N^{-2}): \quad \frac{1}{r^2}\partial_\Theta{}^2\Phi_4 = -\frac{2}{r^2}\partial_\theta\partial_\Theta\Phi_3 + (\mathcal{L} - E_0)\Phi_2 - E_1\Phi_1 - E_2\Phi_0. \tag{4.17}$$

B. Construction of the Multiple Scale Expansion

As is typical in perturbation expansions, we must solve a hierarchy of inhomogeneous linear equations that have a fixed linear operator to invert and a varying inhomogeneous term. Each member of the hierarchy is of the form

$$\frac{1}{r^2}\partial_\Theta{}^2 F = G(r,\ \theta,\ \Theta). \tag{4.18}$$

A necessary and sufficient condition for solvability in the space of 2π periodic in Θ functions is

$$\int_0^{2\pi} G(r,\ \theta,\ p)\mathrm{d}p = 0. \tag{4.19}$$

We now proceed with a term by term construction of the perturbation expansion.

$\mathcal{O}(N^2)$ terms:

$$\frac{1}{r^2}\partial_\Theta{}^2\Phi_0 = 0. \tag{4.20}$$

From this it follows that Φ_0 is independent of the fast phase Θ:

$$\Phi_0(r,\ \theta,\ \Theta) = \Phi_0(r,\ \theta). \tag{4.21}$$

$\mathcal{O}(N)$ terms:

$$-\frac{2}{r^2}\partial_\theta\partial_\Theta\Phi_0 - \frac{1}{r^2}\partial_\Theta{}^2\Phi_1 = 0. \tag{4.22}$$

Using Eq. (4.21) in Eq. (4.22) we obtain

$$\frac{1}{r^2}\partial_\Theta{}^2\Phi_1 = 0. \tag{4.23}$$

Therefore,

$$\Phi_1(r,\ \theta,\ \Theta) = \Phi_1(r,\ \theta). \tag{4.24}$$

Using Eq. (4.24) we find

$\mathcal{O}(1)$ terms:

$$\frac{1}{r^2}\partial_\Theta{}^2\Phi_2 = (\mathcal{L} - E_0)\Phi_0. \tag{4.25}$$

Equation (4.25) has a solution within the space of 2π periodic in Θ functions if and only if the following solvability condition holds:

$$(\mathcal{L}_{\mathrm{av}} - E_0)\Phi_0 = 0. \tag{4.26}$$

Here, $\mathcal{L}_{\mathrm{av}}$ and V_{av} denote, respectively, the average operator and potential with respect to the fast angular dependence. They are given by

$$\mathcal{L}_{\rm av} = -\Delta_\perp + V_{\rm av} = -\Delta_r - \frac{1}{r^2}\partial_\theta{}^2 + V_{\rm av}(r,\ \theta),$$

$$V_{\rm av}(r,\ \theta) = \frac{1}{2\pi}\int_0^{2\pi} V(r,\ \theta,\ p)\mathrm{d}p. \tag{4.27}$$

Note that $\mathcal{L} - \mathcal{L}_{\rm av} = V - V_{\rm av}$.

We fix $[\Phi_0(r,\ \theta),\ E_0]$ to be a scattering resonance pair, an outgoing solution and its associated complex eigenvalue. Since Φ_0 satisfies Eq. (4.26), the inhomogeneous equation (4.25) can be put into a simpler form:

$$\frac{1}{r^2}\partial_\Theta{}^2\Phi_2 = [V(r,\ \theta,\ \Theta) - V_{\rm av}(r,\ \theta)]\Phi_0(r,\ \theta). \tag{4.28}$$

We express the solution of Eq. (4.28) in the form

$$\Phi_2 = \Phi_2{}^{(p)}(r,\ \theta,\ \Theta) + \Phi_2{}^{(h)}(r,\ \theta), \tag{4.29}$$

where $\Phi_2{}^{(p)}(r,\ \theta,\ \Theta)$ and $\Phi_2{}^{(h)}(r,\ \theta)$ are, respectively, a particular solution of mean zero and a homogeneous solution of Eq. (4.28), which is to be determined at higher order in N^{-1}. That $\Phi_2{}^{(p)}(r,\ \theta,\ \Theta)$ can be chosen to be 2π periodic in Θ follows from the mean zero property of $V(r,\ \theta,\ \Theta) - V_{\rm av}(r,\ \theta)$. Also, $\Phi_2{}^{(p)}$ is mean zero in Θ because the constant term in its Fourier expansion is included in $\Phi_2{}^{(h)}$. To compute $\Phi_2{}^{(p)}$, we expand $V(r,\ \theta,\ \Theta) - V_{\rm av}(r,\ \theta)$ in a Fourier series in Θ:

$$V(r,\ \theta,\ \Theta) - V_{\rm av}(r,\ \theta) = \sum_{|j|\geqslant 1} \eta_j(r,\ \theta)\exp(ij\Theta). \tag{4.30}$$

We have

$$\begin{aligned}\Phi_2{}^{(p)}(r,\ \theta,\ \Theta) &= \partial_\Theta{}^{-2}[V(r,\ \theta,\ \Theta) \\ &\quad - V_{\rm av}(r,\ \theta)]r^2\Phi_0(r,\ \theta) \\ &= \sum_{|j|\geqslant 1} (ij)^{-2}\eta_j(r,\ \theta)\exp(ij\Theta)r^2\Phi_0(r,\ \theta).\end{aligned} \tag{4.31}$$

$\mathcal{O}(N^{-1})$ terms:

$$\begin{aligned}\frac{1}{r^2}\partial_\Theta{}^2\Phi_3 &= -\frac{2}{r^2}\partial_\theta\partial_\Theta\Phi_2 + (\mathcal{L} - E_0)\Phi_1 - E_1\Phi_0 \\ &= -\frac{2}{r^2}\partial_\theta\partial_\Theta\Phi_2{}^{(p)} + (\mathcal{L} - E_0)\Phi_1 - E_1\Phi_0.\end{aligned} \tag{4.32}$$

The solvability condition becomes

$$(\mathcal{L}_{\rm av} - E_0)\Phi_1 = E_1\Phi_0, \tag{4.33}$$

which we satisfy by taking $E_1 = 0$ and $\Phi_1 \equiv 0$. Using the mean zero property of $\Phi_2{}^{(p)}$, we observe that Eq. (4.32) becomes

$$\partial_\Theta\Phi_3(r,\ \theta,\ \Theta) = -2\partial_\theta\Phi_2{}^{(p)}(r,\ \theta,\ \Theta). \tag{4.34}$$

$\mathcal{O}(N^{-2})$ terms:

Using $E_1 = 0$, $\Phi_1 \equiv 0$, and Eq. (4.34) to solve for Φ_3 in terms of $\Phi_2{}^{(p)}$, at this order we find that

$$\begin{aligned}\frac{1}{r^2}\partial_\Theta{}^2\Phi_4 &= \frac{4}{r^2}\partial_\theta{}^2\Phi_2{}^{(p)} + (\mathcal{L} - E_0)\Phi_2 - E_2\Phi_0 \\ &= \left(\mathcal{L} - E_0 + \frac{4}{r^2}\partial_\theta{}^2\right)\Phi_2{}^{(p)} \\ &\quad + (\mathcal{L} - E_0)\Phi_2{}^{(h)} - E_2\Phi_0 \\ &= \left(\mathcal{L}_{\rm av} - E_0 + \frac{4}{r^2}\partial_\theta{}^2\right)\Phi_2{}^{(p)} \\ &\quad + (\mathcal{L} - \mathcal{L}_{\rm av})\Phi_2{}^{(h)} + (\mathcal{L}_{\rm av} - E_0)\Phi_2{}^{(h)} \\ &\quad - E_2\Phi_0 + (\mathcal{L} - \mathcal{L}_{\rm av})\Phi_2{}^{(p)}.\end{aligned} \tag{4.35}$$

The first two terms on the right-hand side of Eq. (4.35) have zero average in Θ. Therefore, the solvability condition for Φ_4 becomes

$$\begin{aligned}(\mathcal{L}_{\rm av} - E_0)\Phi_2{}^{(h)} &= E_2\Phi_0 - \frac{1}{2\pi}\int_0^{2\pi}(\mathcal{L} - \mathcal{L}_{\rm av})\Phi_2{}^{(p)}\mathrm{d}p \\ &= E_2\Phi_0 - \frac{1}{2\pi}\int_0^{2\pi}[V(r,\ \theta,\ p) \\ &\quad - V_{\rm av}(r,\ \theta)]\Phi_2{}^{(p)}(r,\ \theta,\ p)\mathrm{d}p \\ &= \left\{E_2 + \frac{r^2}{2\pi}\int_0^{2\pi}|\partial_p{}^{-1}[V(r,\ \theta,\ p) \right. \\ &\quad \left. - V_{\rm av}(r,\ \theta)]|^2\mathrm{d}p\right\}\Phi_0(r,\ \theta),\end{aligned} \tag{4.36}$$

where we used Eq. (4.31) and where $\partial_p{}^{-1}$ denotes the mean-zero antiderivative. We seek an outgoing solution of Eq. (4.36). This determines E_2 and therewith the expansion for the scattering resonance (effective index) through order N^{-2}.

In Section 5 we use this truncated expansion to obtain the complex effective indices (scattering resonances) for various structures numerically. The details of the implementation are set forth in Section 7. In particular, we derive an explicit expression for E_2 [see Eqs. (7.10), (7.17), and (7.18)] for the class of N-fold symmetric waveguides.

5. NUMERICAL SIMULATIONS FOR SELECTED STRUCTURES

We now illustrate the theory of the preceding section with numerical calculations performed for several classes of structures. The details of the implementation are set forth in Section 7. The three classes of structures we consider are:

example 1: a ring of circular air holes (Fig. 2),
example 2: an annulus of air supported with glass webs (Fig. 3), and
example 3: a subset of a hexagonal lattice (Fig. 4).

We identify individual leaky modes or scattering resonances of these structures by using the LP_{lm} (linearly polarized) notation[19] appropriate for solutions of the scalar wave equation. Usually this notation applies to guided

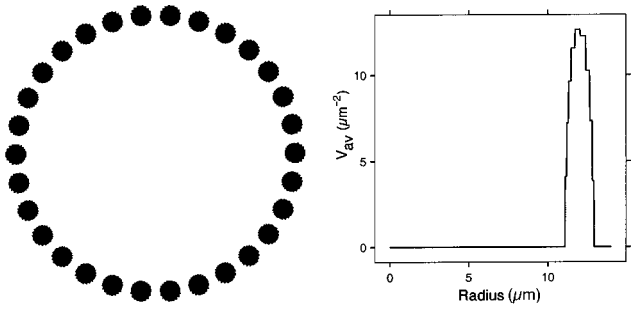

Fig. 2. (a) Ring of $N = 30$ air holes approximated by a simple layered structure with 11 layers. The ratio $R_{\text{hole}}/R_{\text{ring}}$ of the hole radius to the ring radius is $0.7\pi/N$. (b) The averaged potential V_{av} with $R_{\text{ring}} = 12\ \mu$m.

modes, but no ambiguity will result as none of the structures we consider supports guided modes. The subscript $l \in \{0, 1, 2,...\}$ refers to the angular dependence $\exp(il\theta)$ of solutions to the averaged equation, whereas $m \in \{1, 2, 3,...\}$ indicates the collection of leaky modes with fixed l. This collection is ordered by $\Re n_{\text{eff}}$, with $m = 1$ corresponding to the largest such value (when this rule is applied to guided modes, the usual meaning of m as counting the number of nodes in the radial wave function is recovered). In the figures we use distinct plotting symbols to represent different values of l; the various values of m for fixed l are not explicitly displayed but can be inferred from the monotonic relationship between m and $\Re n_{\text{eff}}$.

Examples 1 and 2. The geometries of examples 1 and 2 were varied to produce a total of 30 different structures between them. The ring of holes was scaled to three different core sizes, whereas the annulus with webs was scaled to three different radii for each of two different air-fill fractions and three different periodicities $2\pi/N$. We approximated each of the structures by a simple layered potential, as described in subsection 7.B. (The web-supported annulus depicted in Fig. 3 is a simple layered structure without approximation.) In all the examples, the refractive index of glass was taken to be 1.45 and the holes were assumed to be empty. The calculations were all performed at $\lambda_{\text{fs}} = 1.55\ \mu$m. All these structures support only continuous spectrum, so we report on the complex eigenvalues associated with resonances of the structures.

We computed the following sets of resonances for the rings of circles and webbed structures depicted in Figs. 2 and 3. We restricted attention to leaky mode solutions of the averaged structure with effective indices $\Re n_{\text{eff}} \in [1.41, 1.45]$, attenuation coefficients less than approximately 2 dB/mm, and angular index $l \in \{0, 1, 2, 3\}$. To express these quantities in our notation, note from Eqs. (2.3) that

$$\beta = (k^2 n_g^{\,2} - E)^{1/2} \tag{5.1}$$

and that the effective index is given by

$$n_{\text{eff}} = k^{-1}\beta. \tag{5.2}$$

Also, attenuation γ (in dB/cm if β has units of $1/\mu$m) of a leaky mode is given by

$$\gamma = \frac{2 \times 10^5}{\ln(10)} \Im\beta. \tag{5.3}$$

The factor of 2 in Eq. (5.3) is due to the definition of γ as the attenuation coefficient for intensity rather than field amplitude. Once we found this set of leaky modes of the averaged potential, we computed the leading order corrections E_2 to the leading order energies E_0.

The results for the three scaled rings of circles (Fig. 2) are presented in Fig. 5; those for the three scalings and two air-fill fractions along with various values of periodicity N of the ring of air wedges are presented in Fig. 6.

We also computed resonances of a structure of the type shown in Fig. 3 with $R_{\text{in}} = 1\ \mu$m, $R_{\text{out}} = 2\ \mu$m for fill fractions $f = 0.8$, 0.9, and 1, with $N = 3$ and $N = 6$ holes. The calculations were performed for free-space wavelengths λ_{fs} ranging from 1 to 2 μm. The structure with $f = 1$ is an idealized ring of air with no supporting structure. In Fig. 7 we compare the results of our theory with parallel calculations[6] performed by a Fourier decomposition algorithm. We observe that the two methods agree exactly for the $f = 1$ case, as they should. Additionally, in all cases our method agrees with the Fourier calculation as $\lambda_{\text{fs}} \to 2\ \mu$m. Even for smaller λ_{fs} the agreement is quite good except for the $f = 0.8$, $N = 3$ case, which is not surprising given the small value of N and the fact that the width of the ring is equal to the smallest free-space wavelength considered. The plots

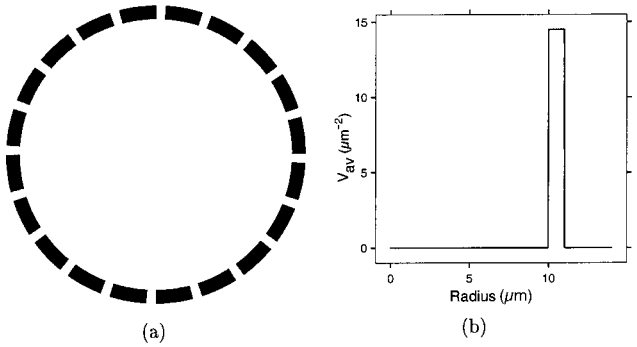

Fig. 3. (a) Ring of air wedges supported by $N = 20$ webs of glass. The ratio $R_{\text{in}}/R_{\text{out}}$ of the outer radii of the annulus is 10/11, whereas the air-fill fraction within the annulus is $f = 0.8$. (b) The averaged potential V_{av} with $R_{\text{in}} = 10\ \mu$m.

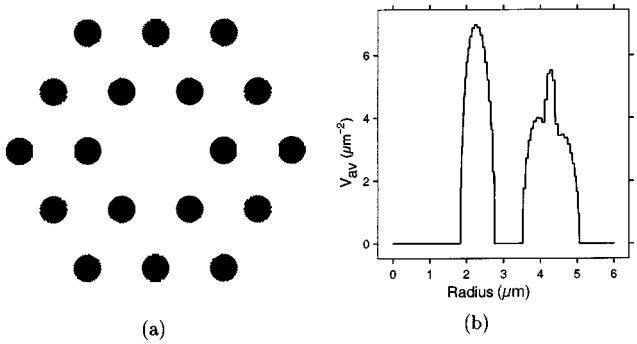

Fig. 4. (a) Eighteen-hole subset of a hexagonal lattice ($N = 6$) with interhole spacing $\Lambda = 2.3\ \mu$m and hole radius $R_{\text{hole}} = 0.46\ \mu$m, approximated by a simple layered structure with $L = 51$ layers. (b) The averaged potential V_{av} in units of μm^{-2} versus radius in units of micrometers.

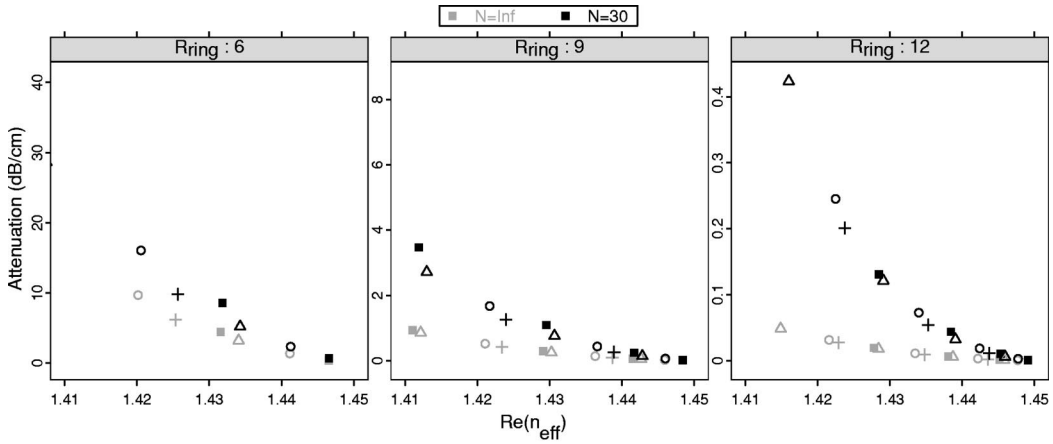

Fig. 5. Effective indices and attenuation coefficients of a set of least-lossy resonances with $l \in \{0, 1, 2, 3\}$ of the structure depicted in Fig. 2, scaled to three different ring radii. The plotting symbol encodes angular index l: ■, ○, △, + correspond to $l = 0, 1, 2, 3$. The results of the averaged structure are labeled $N = \infty$.

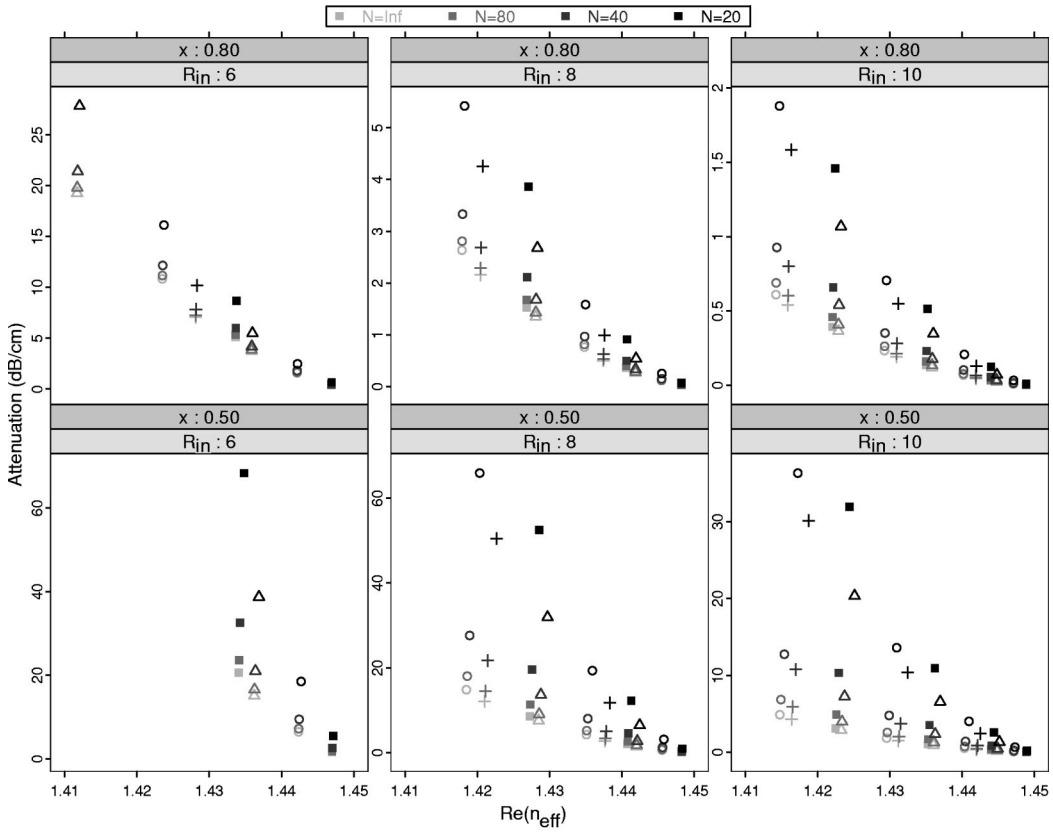

Fig. 6. Effective indices and attenuation coefficients of a set of least-lossy resonances with $l \in \{0, 1, 2, 3\}$ of the structure depicted in Fig. 3 for two choices of fill fraction x and three different radii. The plotting symbol encodes the angular index l: ■, ○, △, + correspond to $l = 0, 1, 2, 3$; the shade of gray encodes periodicity N. The results of the averaged structure are labeled $N = \infty$.

displayed in Fig. 7 are consistent with the expectation that approximation by the homogenization expansion improves (a) for fixed λ_{fs} and increasing N as well as (b) for fixed N and λ_{fs} increasing.

The dashed curves in Fig. 7 display the attenuations of the averaged structures, without the $\mathcal{O}(N^{-2})$ correction. The necessity of including these corrections is evident, although the effect in these structures is not as dramatic as in some of the other structures we consider, including that of example 3 below.

Another result reported in Ref. 6 is the effective index of the first excited state above the fundamental (the LP_{11} state) for the $f = 0.9$, $N = 3$ structure at $\lambda_{fs} = 1.55$ μm. In Table 1 we compare the results of the Fourier method with truncations of our homogenization expansion to one and two terms for both the fundamental and the first ex-

cited leaky modes. We note that the one-term (averaged theory) truncation predicts the real part of the effective index well, agreeing with Ref. 9 but again, the $\mathcal{O}(N^{-2})$ corrections are necessary to obtain good agreement of the attenuation rates.

Example 3. Finally, we consider the structure depicted in Fig. 4. This is an 18-hole subset of a hexagonal lattice ($N = 6$) with interhole spacing $\Lambda = 2.3$ μm and hole radius $R_{\text{hole}} = 0.46$ μm. We found that the fundamental (LP_{01}) resonance has a leakage rate of 14 dB/cm, whereas that of the averaged structure was 0.92 dB/cm. By comparison, the solution to the full vector problem by use of a multipole method with outgoing radiation conditions[4] results in a rate of 16 dB/cm. In this example, the effect of the $N^{-2}E_2$ microstructure correction on the leakage rates is even more apparent than in example 2. However, we cannot say how much of the discrepancy between Ref. 4 and ours is due to vector effects and how much is due to the other approximations in our method.

6. CONVERGENCE AS $N \to \infty$

Here we describe a consistency check on our implementation of the scheme described in subsection 4.B for simple layered potentials; see subsection 7.B. We compute the first nontrivial corrections $N^{-2}\Phi_2$ and $N^{-2}E_2$ to the field and energy, respectively, in Eqs. (4.12) and express the field and energy as our approximation plus error terms:

$$\Phi = \Phi_0 + \frac{1}{N^2}\Phi_2 + \Phi_3{}^{(N)},$$

$$E = E_0 + \frac{1}{N^2}E_2 + E_3{}^{(N)}. \tag{6.1}$$

We consider by how much the mode equation (3.1) is not satisfied by the first two terms of the expansion in Eqs. (6.1). Therefore, we define the residual as

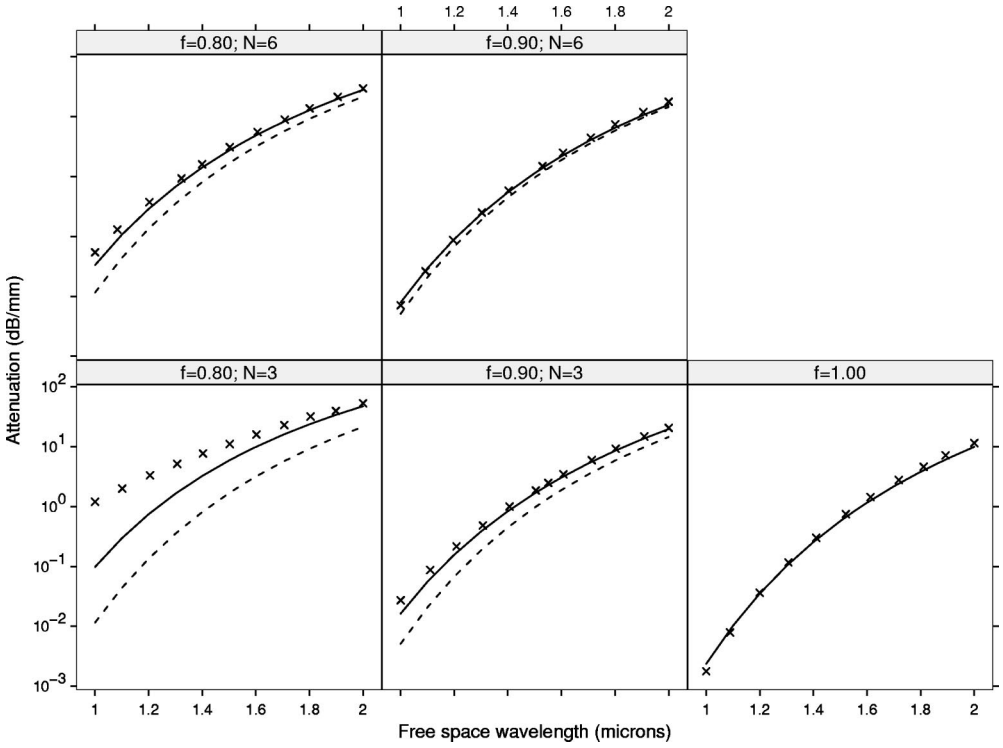

Fig. 7. Attenuation of the lowest-order (fundamental or LP_{01}) resonance for a structure of the type shown in Fig. 3 with $R_{\text{in}} = 1$ μm, $R_{\text{out}} = 2$ μm for fill fractions $f = 0.8$, 0.9, and 1 with $N = 3$ and $N = 6$ holes. The calculations were performed for free-space wavelengths λ_{fs} ranging from 1 to 2 μm. The solid curves represent the attenuations computed according to the methods outlined in the text, including the $\mathcal{O}(N^{-2})$ corrections, the dashed curves represent the attenuations of the averaged structure, and the x corresponds to the results presented in Fig. 3(a) of Ref. 6.

Table 1. Comparison of Results for the First Two Leaky Modes of a Ring of Air Wedges[a]

	Zero-Order Homogenization		Second-Order Homogenization		Fourier	
Mode	n_{eff}	Attenuation	n_{eff}	Attenuation	n_{eff}	Attenuation
LP_{01}	$1.3712 + 0.0000387i$	1.36	$1.3727 + 0.0000644i$	2.27	$1.365 + 0.000071i$	2.48
LP_{11}	$1.2468 + 0.000436i$	15.3	$1.2515 + 0.000832i$	29.3	$1.255 + 0.00075i$	27

[a] With $R_{\text{in}} = 1$ μm, $R_{\text{out}} = 2$ μm, fill fraction $f = 0.9$, and $N = 3$ holes. The effective indices and attenuations (in dB/mm) of the leading term (averaged) and of the two-term truncation of the homogenization expansion are compared with that of the Fourier expansion.[6,18]

$$F_{\rm res} \equiv \left[-\Delta + V - \left(E_0 + \frac{1}{N^2} E_2 \right) \right] \left(\Phi_0 + \frac{1}{N^2} \Phi_2 \right). \tag{6.2}$$

Substituting Eqs. (6.1) into Eq. (3.1), we find that the residual is given by

$$F_{\rm res} = {E_3}^{(N)} \left[\Phi_0 + \frac{1}{N^2} \Phi_2 + {\Phi_3}^{(N)} \right] - \left[\Delta + V - \left(E_0 + \frac{1}{N^2} E_2 \right) \right] {\Phi_3}^{(N)}. \tag{6.3}$$

We expect $F_{\rm res}$ to be of the order of N^{-1} because ${\Phi_3}^{(N)}$ and ${E_3}^{(N)}$ are formally of the order of N^{-3}, and the Laplacian in Eq. (6.3), when acting on the fast dependence, gives a factor of N^2. Indeed, expanding $F_{\rm res}$ in powers of $1/N$, we find that, when $l > 0$, the leading term ${F_{\rm res}}^{(1)}$ is the $\mathcal{O}(1/N)$ term

$${F_{\rm res}}^{(1)} = \frac{1}{Nr^2} \partial_\Theta{}^2 \Phi_3 . \tag{6.4}$$

This could be simplified by use of Eqs. (4.34) and (4.31):

$${F_{\rm res}}^{(1)} = -\frac{2}{N} (\partial_\theta \Phi_0) [\partial_\Theta{}^{-1} (V - V_{\rm av})]. \tag{6.5}$$

Therefore, when $l > 0$, we expect that, as $N \to \infty$,

$$F_{\rm res} \to {F_{\rm res}}^{(1)} \sim \mathcal{O}\left(\frac{1}{N} \right), \quad F_{\rm res} - {F_{\rm res}}^{(1)} \sim \mathcal{O}\left(\frac{1}{N^2} \right). \tag{6.6}$$

When $l = 0$, it follows that $\Phi_0 = \Phi_0(r)$, $\partial_\theta \Phi_0$ vanishes, and the leading behavior of the residual is of higher order in $1/N$.

Since the potential V or its derivatives can have discontinuities, it is problematic to compute $F_{\rm res}$ by using Eq. (6.3); it is possible that ${\Phi_2}^{(p)}$ is discontinuous as a function of r. We therefore interpret Eq. (6.3) as holding in the weak sense or sense of distributions and integrate both sides against a radial test function $\phi_R(r)$ of compact support. This allows us to move the radial part of the Laplacian over to act on ϕ_R and to define the *weak residual* as

$${F_{\rm res}}^{(\rm weak)}(\theta) = \int_0^\infty r \, {\rm d}r \left[-\phi_R{}'' - \frac{1}{r} \phi_R{}' - \phi_R \frac{1}{r^2} \partial_\theta{}^2 + \phi_R \left(V - E_0 - \frac{1}{N^2} E_2 \right) \right] \times \left(\Phi_0 + \frac{1}{N^2} \Phi_2 \right), \tag{6.7}$$

and its leading behavior in $1/N$ as

$${F_{\rm res}}^{(\rm weak,1)}(\theta) = -\frac{2}{N} \int_0^\infty r \, {\rm d}r \, \phi_R (\partial_\theta \Phi_0) [\partial_\Theta{}^{-1} (V - V_{\rm av})]. \tag{6.8}$$

We computed Eqs. (6.7) and (6.8) for the structure of example 2 (Fig. 3), with $R_{\rm in} = 10$ μm and $R_{\rm out} = 11$ μm, for the $\rm LP_{11}$ leaky mode. We allowed N to vary from 20 to 22,000. The results are presented in Fig. 8. The solid line in Fig. 8(a) represents $\| {F_{\rm res}}^{(\rm weak)}(\theta) - {F_{\rm res}}^{(\rm weak,1)}(\theta) \|_\infty$ as a function of N. The scales are logarithmic on both axes, so the slope of -2 verifies that the first term in (6.6) holds over the entire range considered. The dashed curve in Fig. 8(a) represents $\| {F_{\rm res}}^{(\rm weak)}(\theta) \|_\infty$; we see that the slope changes from -2 to -1 at around $N = 1000$, which again verifies terms (6.6).

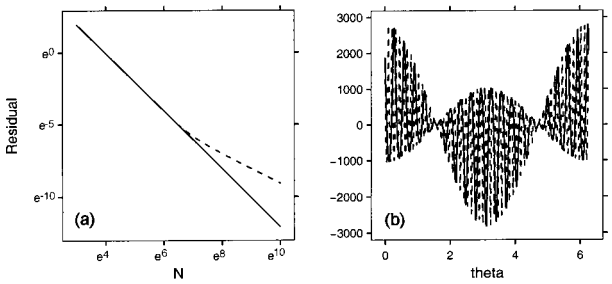

Fig. 8. Results of weak residual calculation: (a) $\| {F_{\rm res}}^{(\rm weak)}(\theta) - {F_{\rm res}}^{(\rm weak,1)}(\theta) \|_\infty$ (solid line) and $\| {F_{\rm res}}^{(\rm weak)}(\theta) \|_\infty$ (dashed curve); (b) $N^2 \Re[{F_{\rm res}}^{(\rm weak)}(\theta) - {F_{\rm res}}^{(\rm weak,1)}(\theta)]$ for $N = 20$ (solid curve) and $N = 54$ (dashed curve).

Figure 8(b) shows the pointwise behavior of the weak residuals by plotting $N^2 \Re[{F_{\rm res}}^{(\rm weak)}(\theta) - {F_{\rm res}}^{(\rm weak,1)}(\theta)]$ versus θ for $N = 20$ and $N = 54$. We observe that the envelope of the residuals is invariant after scaling by N^2, suggesting that the N^{-2} term dominates the residual after the leading term is subtracted, even for these moderate values of N. This behavior persists for all N we considered up to $N = 22{,}000$.

7. IMPLEMENTATION OF HOMOGENIZATION EXPANSION

In this section we outline the procedure used to obtain the simulation results in Section 6. We specialize to the case of a potential with no slow angular dependence, so $V(r, \theta, \Theta) = V(r, \Theta)$. In this case, the potential has an N-fold symmetry. First, in Subsection 7.A, we sketch the expansion of solutions to the resonance problem summarized in the homogenization expansion in Section 4 with no additional assumptions. This discussion pertains to N-fold symmetric microstructure whose individual microfeatures have arbitrary geometry. Our strategy then is to approximate a general microstructure potential V by a simple layered potential in Subsection 7.B. For simple layered potentials, analytic expressions can be obtained that facilitate the numerical computations.

A. General Structures

The angular average potential is a radial function $V_{\rm av} = V_{\rm av}(r)$. We let $\Phi_0(r, \theta) = f(r) \exp(il\theta)$, where l is an integer. Then $f(r)$ satisfies

$$\left[-\Delta_r + \frac{l^2}{r^2} + V_{\rm av}(r) - E_0 \right] f(r) = 0. \tag{7.1}$$

A solution of the resonance problem is the pair $[f(r), E_0]$, such that $f(r)$ is a nonsingular solution of Eq. (7.1) that satisfies an outgoing radiation condition at $r = \infty$; see Eq. (3.4). As noted in Section 3, E_0 is complex with $\Im E_0 < 0$. In general, the existence of solutions to the resonance problem is a subtle technical problem. In Sub-

section 7.B we analyze the problem in detail for the particular class of simple layered structures that we define there. In this section, we posit the existence of a solution $[f(r), E_0]$. Note that since $V_{\rm av}(r) = 0$ for $r \geqslant r_*$,

$$f(r) = k_* H_l^{(1)}(\sqrt{E_0} r), \quad r \geqslant r_* \tag{7.2}$$

for some constant k_*.

Next we calculate the leading order correction $N^{-2}\Phi_2$ by our perturbation scheme. In the separable case, the equation for ${\Phi_2}^{(h)}$ is of the form

$$(\mathcal{L}_{\rm av} - E_0){\Phi_2}^{(h)} = [E_2 + Q(r)]\Phi_0, \tag{7.3}$$

where $Q(r)$ has compact support. Since $\Phi_0(r, \theta) = f(r)\exp(il\theta)$, all the Fourier modes of ${\Phi_2}^{(h)}(r, \theta)$ except the lth mode vanish and so we define ${\Phi_2}^{(h)}(r, \theta) = U(r)\exp(il\theta)$ and consider the equation

$$\left[-\Delta_r + \frac{l^2}{r^2} + V_{\rm av}(r) - E_0\right] U(r) = [E_2 + Q(r)]f(r). \tag{7.4}$$

Note that, from Eq. (2.5), both Q and $V_{\rm av}$ are zero for $r \geqslant r_*$, and we have

$$\left(-\Delta_r + \frac{l^2}{r^2} - E_0\right) U(r) = E_2 f(r), \quad r \geqslant r_*. \tag{7.5}$$

We proceed with the solution of the inhomogeneous problem in Eq. (7.4) for $r \geqslant 0$ and then obtain an expression for E_2 by imposing the outward-going radiation condition.

We have assumed that V is regular at the origin. We let $\tilde{y}_1(r)$ denote the solution to the homogeneous equation associated with Eq. (7.4) that is regular at $r = 0$ and $\tilde{y}_2(r)$ denote an independent solution, which together with $\tilde{y}_1$ spans the solution set. Then $\tilde{y}_1(r) \propto r^l$ and $\tilde{y}_2(r) \propto r^{-l}$ if $l > 0$, or $\tilde{y}_1(r) \propto \ln(r)$ if $l = 0$. For $r > r_*$, an appropriate set of homogeneous solutions of Eq. (7.5) is in terms of Hankel functions $H_l^{(j)}(\sqrt{E_0} r)$, $j = 1, 2$. $H_l^{(1)}$ satisfies the outward-going radiation condition at infinity and $H_l^{(2)}$ the inward-going radiation condition at infinity.

A particular solution of Eq. (7.4) can be constructed by variation of parameters by use of these homogeneous solutions in the intervals $R_{\rm in} = [0, r_*]$ and $R_{\rm out} = (r_*, \infty)$. We define $\mathcal{G}_{\rm in}[F]$ to be a choice of particular solution of

$$\left[-\Delta_r + \frac{l^2}{r^2} + V_{\rm av}(r) - E_0\right] \mathcal{G}_{\rm in}[F] = F(r), \quad 0 \leqslant r < r_* (r \in R_{\rm in}), \tag{7.6}$$

and define $\mathcal{G}_{\rm out}[F]$ to be a choice of particular solution of

$$\left(-\Delta_r + \frac{l^2}{r^2} - E_0\right) \mathcal{G}_{\rm out}[F] = F(r), \quad r_* \leqslant r (r \in R_{\rm out}). \tag{7.7}$$

We then have

$$U(r) = E_2 \mathcal{G}_{\rm in}[f](r) + \mathcal{G}_{\rm in}[Qf](r) \tag{7.8}$$

for $R_{\rm in}$ and

$$U(r) = \xi_* H_l^{(1)}(\sqrt{E_0} r) + \eta_* H_l^{(2)}(\sqrt{E_0} r) + E_2 \mathcal{G}_{\rm out}[f](r) \tag{7.9}$$

for $R_{\rm out}$, where the coefficients ξ_* and η_* are determined by imposing continuity of U and $\partial_r U$ at $r = r_*$:

$$\begin{aligned}\begin{bmatrix}\xi_*(E_2)\\ \eta_*(E_2)\end{bmatrix} &= E_2 \mathscr{Y}^{-1}(r_*) \\ &\quad \times \begin{pmatrix} \mathcal{G}_{\rm in}[f](r_*) - \mathcal{G}_{\rm out}[f](r_*) \\ {E_0}^{-1/2}\{\partial \mathcal{G}_{\rm in}[f](r_*) - \partial \mathcal{G}_{\rm out}[f](r_*)\}\end{pmatrix} \\ &\quad + \mathscr{Y}^{-1}(r_*)\begin{Bmatrix} \mathcal{G}_{\rm in}[Qf](r_*) \\ {E_0}^{-1/2}\partial \mathcal{G}_{\rm in}[Qf](r_*)\end{Bmatrix},\end{aligned} \tag{7.10}$$

with

$$\mathscr{Y}(r) = \begin{bmatrix} H_l^{(1)}(\sqrt{E_0} r) & H_l^{(2)}(\sqrt{E_0} r) \\ \partial_s H_l^{(1)}(\sqrt{E_0} r) & \partial_s H_l^{(2)}(\sqrt{E_0} r)\end{bmatrix}.$$

With ξ_* and η_* given by Eq. (7.10), Eqs. (7.8) and (7.9) define a nonsingular solution of Eq. (7.4). It remains to impose a radiation condition at $r = \infty$. Consider $U(r)$ for $r \geqslant r_*$. Let

$$z = \sqrt{E_0} r, \quad z_* = \sqrt{E_0} r_*, \quad G(z) = U[r(z)].$$

Then, Eq. (7.5) becomes

$$z^2 G'' + zG' + (z^2 - l^2)G = \frac{E_2}{E_0} k_* z^2 H_l^{(1)}(z), \quad r(z) \geqslant r_*. \tag{7.11}$$

Equations (7.9) and (7.2) yield

$$\begin{aligned} G(z) &= U[r(z)] \\ &= \xi_*(E_2) H_l^{(1)}(z) + \eta_*(E_2) H_l^{(2)}(z) \\ &\quad + \frac{E_2}{E_0} k_* \mathcal{G}_{\rm out}[H_l^{(1)}](z). \end{aligned} \tag{7.12}$$

$\mathcal{G}_{\rm out}$ can be constructed by variation of parameters. A particular solution is

$${\xi_*}^{(p)}(z) H_l^{(1)}(z) + {\eta_*}^{(p)}(z) H_l^{(2)}(z),$$

where

$${\xi_*}^{(p)}[h](z) = -\int_{z_*}^{z} \frac{H_l^{(2)}(\zeta) h(\zeta)}{\zeta^2 W\{H_l^{(1)}, H_l^{(2)}\}} \, d\zeta, \tag{7.13}$$

$${\eta_*}^{(p)}[h](z) = +\int_{z_*}^{z} \frac{H_l^{(1)}(\zeta) h(\zeta)}{\zeta^2 W\{H_l^{(1)}, H_l^{(2)}\}} \, d\zeta. \tag{7.14}$$

Therefore,

$$\begin{aligned} \mathcal{G}_{\rm out}[F](z) &= \{{\xi_*}^{(p)}[\zeta^2 F](z) H_l^{(1)}(z) \\ &\quad + {\eta_*}^{(p)}[\zeta^2 F](z) H_l^{(2)}(z)\}, \end{aligned} \tag{7.15}$$

Using Eq. (7.15) in Eq. (7.12) we obtain

$$\begin{aligned} G(z) &= U[r(z)] \\ &= \xi_*(E_2) H_l^{(1)}(z) + \eta_*(E_2) H_l^{(2)}(z) \\ &\quad - \frac{i\pi}{4} \frac{E_2}{E_0} k_* \int_{z_*}^{z} H_l^{(2)}(\zeta) H_l^{(1)}(\zeta) \zeta \, d\zeta H_l^{(1)}(z) \\ &\quad + \frac{i\pi}{4} \frac{E_2}{E_0} k_* \int_{z_*}^{z} [H_l^{(1)}(\zeta)]^2 \zeta \, d\zeta H_l^{(2)}(z). \end{aligned} \tag{7.16}$$

Note that $\xi_*(E_2)$ and $\eta_*(E_2)$ are determined by the continuity conditions at $r = r_*$ and are given by Eq. (7.10). The condition that determines E_2 is that the incoming

part of $G(z)$ be identically zero. Derivation of this condition on E_2 requires the use of certain integral identities that involve Hankel functions.

Note that both terms in Eq. (7.16) that are proportional to $H_l^{(1)}$ are outgoing, as can be seen when we refer to their asymptotic forms. From Ref. 20 we have

$$\int \zeta[H_l^{(j)}(\zeta)]^2\,\mathrm{d}\zeta = \frac{\zeta^2}{2}\{[H_l^{(j)}(\zeta)]^2 - H_{l-1}^{(j)}(\zeta) \times H_{l+1}^{(j)}(\zeta)\}.$$

Therefore, the terms in Eq. (7.16) that are proportional to $H_l^{(2)}$ can be written as

$$\begin{aligned}\eta_*(E_2)H_l^{(2)}(z) &+ \frac{ik_*\pi}{4}\frac{E_2}{E_0}\frac{\zeta^2}{2}\{[H_l^{(1)}(\zeta)]^2 \\ &- H_{l-1}^{(1)}(\zeta)H_{l+1}^{(1)}(\zeta)\}|_{z_*}^{z}H_l^{(2)}(z) \\ &= \left(\eta_*(E_2) - \frac{ik_*\pi}{4}\frac{E_2}{E_0}\frac{z_*^2}{2}\{[H_l^{(1)}(z_*)]^2 \right. \\ &\left. - H_{l-1}^{(1)}(z_*)H_{l+1}^{(1)}(z_*)\}\right)H_l^{(2)}(z) \\ &+ \frac{ik_*\pi}{4}\frac{E_2}{E_0}\frac{z^2}{2}\{[H_l^{(1)}(z)]^2 \\ &- H_{l-1}^{(1)}(z)H_{l+1}^{(1)}(z)\}H_l^{(2)}(z).\end{aligned}$$

Again, from the asymptotic form of $H_l^{(1)}$, the latter term is seen to be outgoing at infinity so the condition for E_2 is

$$\eta_*(E_2) - \frac{ik_*\pi}{4}\frac{E_2}{E_0}\frac{z_*^2}{2}\{[H_l^{(1)}(z_*)]^2 - H_{l-1}^{(1)}(z_*)H_{l+1}^{(1)}(z_*)\} = 0. \quad (7.17)$$

We can write $\eta_*(E_2)$ as

$$\eta_*(E_2) = \eta_{*0} + E_2\eta_{*1}, \quad (7.18)$$

where $\eta_{*0,1}$ can be read from the second component of Eq. (7.10). Equations (7.17) and (7.18) give a linear relation for E_2 that can be solved.

B. Simple Layered Structures: Leading Order Resonances

We now outline an implementation of the above scheme for a simple layered structure that we define to be one with potential $V(r, \theta, \Theta)$ that is both independent of the slow angular variable θ and is a simple function of the form

$$V(r, \Theta) = \sum_{i=1}^{L}\sum_{j=1}^{M_i} \mathbf{1}_{[r_i, r_{i+1}]}(r)\mathbf{1}_{[\Theta_j, \Theta_{j+1}]}(\Theta)V_{i,j}, \quad (7.19)$$

where L is the number of radial layers and M_i is the number of angular sectors in one period of the ith layer. $\mathbf{1}_A(\zeta)$ denotes the indicator function of set A, taking the value one for $\zeta \in A$ and zero for $\zeta \notin A$. By definition, $r_1 = 0$, $\Theta_1 = 0$, and $\Theta_{M_i+1} = 2\pi$. The potential in Eq. (7.19) has, as a function of Θ, M_i jumps in layer R_i and, as a function of θ, NM_i jumps in layer R_i. An example of a simple layered approximation to a structure that contains six circular air holes is presented in Fig. 9.

With the definition in Eq. (7.19) of $V(r, \Theta)$, $V_{\mathrm{av}}(r)$ is constant in each region $R_i = [r_i, r_{i+1}]$; equivalently,

$$V_{\mathrm{av}}(r) = V_{\mathrm{av},i}, \quad r \in R_i. \quad (7.20)$$

In the special case where the index profile $n(r, \theta)$ takes on two values of n_g and n_h and $2\pi f_i$ denotes the total angle of annulus R_i occupied by material h, by averaging V in Eqs. (2.3) we have

$$V_{\mathrm{av}}(r) = k^2 f_i[n_g{}^2 - n_h{}^2], \quad r \in R_i. \quad (7.21)$$

In each interval R_i, the radial wave function $f(r)$ can be expressed as a linear combination of Bessel and modified Bessel functions:

$$f(r) = \sigma_i y_1(z(r)) + \tau_i y_2(z(r)), \quad (7.22)$$

where, for $i < L$, the definitions of y_1, y_2, and z depend on the sign of $\Re(E_0 - V_{\mathrm{av}})$. If $\Re(E_0 - V_{\mathrm{av}}) > 0$, then $z = (E_0 - V_{\mathrm{av}})^{1/2}r$, $y_1 = J_l$, and $y_2 = Y_l$; otherwise, $z = (V_{\mathrm{av}} - E_0)^{1/2}r$, $y_1 = I_l$, and $y_2 = K_l$. In the outer region, where $i = L$, we let $z = E_0^{1/2}$, $y_1 = H_l^{(1)}$, and $y_2 = H_l^{(2)}$. The condition that the solution be nonsingular at $r = 0$ implies that

$$\begin{pmatrix}\sigma_1\\ \tau_1\end{pmatrix} = \begin{pmatrix}1\\ 0\end{pmatrix} \quad (7.23)$$

or a multiple thereof. The values of (σ_i, τ_i) in some interval i determine the values $(\sigma_{i+1}, \tau_{i+1})$ by continuity of $f(r)$ and its derivative at the interface. This relationship can be expressed by a transfer matrix[21] $\mathbf{T}_i(E_0)$ that gives rise to the relationship between the coefficients in the outermost layer and those in the innermost layer:

$$\begin{pmatrix}\sigma_L\\ \tau_L\end{pmatrix} = \mathbf{T}(E_0)\begin{pmatrix}\sigma_1\\ \tau_1\end{pmatrix}, \quad (7.24)$$

where

$$\mathbf{T}(E_0) = \mathbf{T}_L(E_0)\cdots\mathbf{T}_3(E_0)\mathbf{T}_2(E_0). \quad (7.25)$$

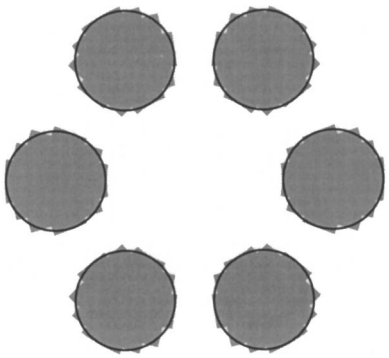

Fig. 9. Example of a simple layered approximation of a structure that contains six circular air holes [see Eq. (7.19)].

The radiation condition is equivalent to the orthogonality of $(0, 1)$ and (σ_L, τ_L). Therefore, the resonance or scattering energies are determined by the following scalar transcendental equation:

$$(0 \quad 1)\mathbf{T}(E_0)\begin{pmatrix}1\\0\end{pmatrix} = 0 \tag{7.26}$$

or equivalently

$$T_{21}(E_0) = 0, \tag{7.27}$$

where T_{kj} denotes the (k, j) entry of matrix $\mathbf{T}(E_0)$.

C. Simple Layered Structures: Microstructure Corrections to Φ_0 and E_0

We now construct the order N^{-2} correction to Φ_0, which is $N^{-2}\Phi_2$, and to E_0, which is $N^{-2}E_2$, for the special case of a simple layered structure; see Eq. (7.19). Note that $\Phi_2 = \Phi_2^{(p)} + \Phi_2^{(h)}$. Here $\Phi_2^{(p)}$ is, in general, given by the Fourier series in Eq. (4.31). When the potential is of the form in Eq. (7.19), $\Phi_2^{(p)}$ can be explicitly calculated, which is done in Appendix A. $\Phi_2^{(h)}$ solves Eq. (4.36) and E_2 is chosen so that Eq. (4.31) has a solution that satisfies the outgoing radiation condition at $r = \infty$. We now focus on the determination of E_2 and $\Phi_2^{(h)}$ in the separable case.

Note that Eq. (4.36) for $\Phi_2^{(h)}$ is of the form

$$(\mathcal{L}_{\mathrm{av}} - E_0)\Phi_2^{(h)} = [E_2 + Q(r)]\Phi_0, \tag{7.28}$$

where $Q(r)$ has compact support; its explicit form for simple structures is presented in Appendix A. Since $\Phi_0(r, \theta) = f(r)\exp(il\theta)$, we define $\Phi_2^{(h)}(r, \theta) = U(r) \times \exp(il\theta)$ and consider the equation

$$\left[-\Delta_r + \frac{l^2}{r^2} + V_{\mathrm{av}}(r) - E_0\right]U(r) = [E_2 + Q(r)]f(r). \tag{7.29}$$

The solution of Eq. (7.29) in region R_q can be written as

$$U_q(r) = U_q^{(p)}[z(r)] + \xi_q y_1[z(r)] + \eta_q y_2[z(r)], \tag{7.30}$$

where the definitions of y_1, y_2, and z are the same as in Eq. (7.22) and $U_q^{(p)}$ denotes a particular solution obtained by variation of the parameters. As above, the coefficients (ξ_{q+1}, η_{q+1}) can be obtained from (ξ_q, η_q) if we impose continuity of $U(r)$ and its derivative at the interface. We omit the details, but note that the transfer matrix formulation from Eq. (7.23) is modified in this case to reflect the presence of a homogeneous term:

$$\begin{pmatrix}\xi\\ \eta\end{pmatrix} = \mathbf{F}_q(E_2) + \mathbf{T}_q\begin{pmatrix}\xi_{q-1}\\ \eta_{q-1}\end{pmatrix}. \tag{7.31}$$

Note that the matrix $\mathbf{T}_q$ does not depend on E_2, although $\mathbf{F}_q$ does.

The solution in the innermost region R_1, $U_1(r)$, must be regular at the origin. Through a choice of particular solution, we can take the homogeneous part of the solution in this region to be identically zero. Then, iteration of Eq. (7.31) yields

$$\begin{bmatrix}\xi_L(E_2)\\ \eta_L(E_2)\end{bmatrix} = \mathbf{F}_L + \mathbf{T}_L\mathbf{F}_{L-1} + \mathbf{T}_L\mathbf{T}_{L-1}\mathbf{F}_{L-2} + \cdots + \mathbf{T}_L\mathbf{T}_{L-1}\cdots\mathbf{T}_3\mathbf{F}_2. \tag{7.32}$$

It remains to impose the radiation condition in outermost region R_L. We note that $Q(r) \equiv 0$ in Eq. (7.28) and that, by construction, Φ_0 is outgoing and thus can be written as

$$\Phi_0(r, \theta) = \sigma_L H_l^{(1)}(\sqrt{E_0}r). \tag{7.33}$$

Therefore, to impose the radiation condition on the correction and thereby obtain E_2, we can use Eq. (7.11) with $k_* = \sigma_L$. We can therefore use the calculations from Subsection 7.B to obtain a particular solution. This gives the equation for E_2:

$$\eta_L(E_2) - \frac{i\sigma_L\pi}{4}\frac{E_2}{E_0}\frac{z_L^2}{2}\{[H_l^{(1)}(z_L)]^2 - H_{l-1}^{(1)}(z_L)H_{l+1}^{(1)}(z_L)\} = 0, \tag{7.34}$$

where

$$\eta_L(E_2) \equiv \eta_{L0} + E_2\eta_{L1} \tag{7.35}$$

is read from Eq. (7.32). We then find E_2 by solving the linear relation in Eqs. (7.34) and (7.35).

8. SUMMARY AND DISCUSSION

We have derived a systematic homogenization expansion for microstructured cylindrical waveguides with transverse N-fold symmetry. The method of derivation, multiple scale analysis, facilitates the removal of fast scales that are due to rapid variations in the microstructure. Therefore, numerical implementation of the expansion does not encounter the intrinsic stiffness associated with problems having large separations of scales. We have implemented the expansion for a number of sample structures and have computed the effective indices of their leaky modes (scattering resonances). Of great importance are the imaginary parts of the effective indices that correspond to the leakage rates that result from a combination of propagation and tunneling losses. In contrast to the real parts of the effective indices, these leakage rates are sensitive to the geometry of the microstructure for low-index (air) holes.

The homogenization expansion can be viewed in the more general context of perturbation theory of scattering resonances for wave equations with rapidly varying perturbations that are not necessarily pointwise small. In quantum mechanics, the eigenvalue problem [see Eqs. (1.1)] is referred to as the scattering resonance problem. The complex eigenvalues are called scattering resonances or scattering frequencies whose imaginary parts give the lifetime of elementary particle states. In a forthcoming paper[14] we develop a rigorous perturbation theory of such scattering resonances that is valid for high contrast potentials (arbitrary index contrasts), offers insight into the regime of validity of the homogenization expansion, and provides concrete error bounds for truncated expansion. The theory explains the trends observed in the simulations we reported in Section 5; for example, that our homogenization expansion provides an increasingly accurate approximation of the modes and effective indices for (a) fixed wavelength λ_{fs} and N increasing and (b) fixed N and λ_{fs} increasing. The goal of this forthcoming analytical work is to develop an understanding of the interplay among wavelength, spatial variation of the index con-

trast, and the geometry of the microstructure to determine the propagation properties of microstructure waveguides and, in particular, to determine the regime of validity of the homogenization expansion.

APPENDIX A: CALCULATIONS FOR SIMPLE LAYERED STRUCTURES

We present the expressions needed to compute the leading corrections for Φ_0 and E_0 arising from the microstructure. There are two quantities that we require:

$$\Phi_2{}^{(p)}(r,\theta,\Theta) = r^2\Phi_0(r,\theta)\partial_\Theta{}^{-2}[V(r,\Theta) - V_{\mathrm{av}}(r)], \tag{A1}$$

$$Q(r) = \frac{r^2}{2\pi}\int_0^{2\pi} |\partial_p{}^{-1}[V(r,p) - V_{\mathrm{av}}(r)]|^2 \mathrm{d}p. \tag{A2}$$

The mean-zero antiderivatives in Eqs. (A1) and (A2) are explicitly calculable because of the form of the potential in Eq. (7.19). For $r \in R_i$,

$$\partial_\Theta{}^{-1}[V(r,\Theta) - V_{\mathrm{av}}(r)] = C_1 - V_{\mathrm{av},i}\Theta + \sum_{j=1}^{M_i} \mathbf{1}_{[\Theta_j,\,\Theta_{j+1}]}(\theta)[S_j + V_{i,j}(\Theta - \Theta_j)], \tag{A3}$$

where

$$\partial_\Theta{}^{-2}[V(r,\Theta) - V_{\mathrm{av}}(r)] = C_2 + C_1\Theta - \frac{1}{2}V_{\mathrm{av},i}\Theta^2 + \sum_{j=1}^{M_i} \mathbf{1}_{[\Theta_j,\,\Theta_{j+1}]}(\Theta)\left[T_j + S_j(\Theta - \Theta_j) + \frac{1}{2}V_{i,j}(\Theta - \Theta_j)^2\right], \tag{A5}$$

$$S_j = \sum_{k=1}^{j-1} V_{i,k}(\Theta_{k+1} - \Theta_k) \tag{A4}$$

and the constant C_1 is given below. Integrating once more for $r \in R_i$,

where

$$T_j = \sum_{k=1}^{j-1}\left[S_k(\Theta_{k+1} - \Theta_k) + \frac{1}{2}V_{i,k}(\Theta_{k+1} - \Theta_k)^2\right], \tag{A6}$$

and the constants C_1 and C_2 are given by

$$C_1 = \pi V_{\mathrm{av},i} - T_{M_i+1},$$

$$C_2 = -\pi C_1 + \frac{(2\pi)^2}{6}V_{\mathrm{av},i} - \frac{1}{2\pi}\sum_{j=1}^{M_i}\left(T_j(\Theta_{j+1} - \Theta_j) + \frac{1}{2}S_j(\Theta_{j+1} - \Theta_j)^2 + \frac{1}{6}V_{i,j}(\Theta_{j+1} - \Theta_j)^3\right). \tag{A7}$$

Finally, for $r \in R_i$, the integral in Eq. (A2) evaluates to

$$\frac{1}{2\pi}\int_0^{2\pi} |\partial_p{}^{-1}[V(r,p) - V_{\mathrm{av}}(r)]|^2 \mathrm{d}p = C_1{}^2 + \frac{1}{\pi}C_1 T_{M_i+1} + \frac{1}{2\pi}\sum_{j=1}^{M_i}\left(S_j{}^2(\Theta_{j+1} - \Theta_j) + S_j(V_{i,j} - V_{\mathrm{av},i}) \times (\Theta_{j+1} - \Theta_j)^2 + \frac{1}{3}(V_{i,j} - V_{\mathrm{av},i})^2(\Theta_{j+1} - \Theta_j)^3\right). \tag{A8}$$

ACKNOWLEDGMENTS

The authors thank B. Eggleton, R. Windeler, R. Bise, D. DiGiovanni, and J. Jaspara for introducing them to the subject of microstructured optical fiber and for discussions on physical aspects. The authors also thank R. V. Kohn, G. C. Papanicolaou, T. Salamon, and M. Vogelius for stimulating and informative discussions during the preparation of this study.

The e-mail address for M. I. Weinstein is miw @research.bell-labs.com, and for S. E. Golowich is golowich@research.bell-labs.com.

REFERENCES AND NOTES

1. R. F. Cregan, B. J. Mangan, J. C. Knight, T. A. Birks, P. St. J. Russell, P. J. Roberts, and D. C. Allan, "Single-mode photonic band gap guidance of light in air," Science **285**, 1537–1539 (1999).
2. J. K. Ranka, R. S. Windeler, and A. J. Stentz, "Visible continuum generation in air–silica microstructure optical fibers with anomalous dispersion at 800 nm," Opt. Lett. **25**, 25–27 (2000).
3. J. Jasapara, R. Bise, and R. Windeler, "Chromatic dispersion measurements in a photonic bandgap fiber," in *Optical Fiber Communication*, Vol. 70 of OSA Trends in Optics and Photonics (Optical Society of America, Washington, D.C., 2002).
4. T. P. White, R. C. McPhedran, C. M. de Sterke, L. C. Botten, and M. J. Steel, "Confinement losses in microstructured optical fibers," Opt. Lett. **26**, 1660–1662 (2001).
5. T. M. Monro, D. J. Richardson, N. G. R. Broderick, and P. J. Bennett, "Modeling large air fraction holey optical fibers," J. Lightwave Technol. **18**, 50–56 (2000).
6. L. Poladian, N. A. Issa, and T. M. Monro, "Fourier decomposition algorithm for leaky modes of fibres with arbitrary geometry," Opt. Express **10**, 449–454 (2002).
7. B. J. Eggleton, P. S. Westbrook, C. A. White, C. Kerbage, R. S. Windeler, and G. L. Burdge, "Cladding-mode-resonances in air–silica microstructure optical fibers," J. Lightwave Technol. **18**, 1084–1100 (2000).
8. M. J. Steel and R. M. Osgood, Jr., "Elliptical-hole photonic crystal fibers," Opt. Lett. **26**, 229–231 (2001).
9. A. Argyros, I. M. Bassett, M. A. van Eijkelenborg, M. C. J. Large, J. Zagari, N. A. P. Nicorovici, R. C. McPhedran, and

C. M. de Sterke, "Ring structures in microstructured polymer optical fibers," Opt. Express **9**, 813–820 (2001).
10. A. Bensoussan, J. L. Lions, and G. C. Papanicolaou, *Asymptotic Analysis for Periodic Structures*, Vol. 5 of Studies in Mathematics and Its Applications (North-Holland, Amsterdam, 1978).
11. G. W. Milton, *The Theory of Composites*, Cambridge Monographs on Applied and Computational Mathematics (Cambridge University, Cambridge, England, 2002).
12. F. Santosa and M. Vogelius, "First-order corrections to the homogenized eigenvalues of a periodic composite medium," SIAM (Soc. Ind. Appl. Math.) J. Appl. Math. **53**, 1636–1668 (1993).
13. S. Moskow and M. Vogelius, "First-order corrections to the homogenized eigenvalues of a periodic composite medium: a convergence proof," Proc. R. Soc. Edinburgh Sect. A Math. **127**, 1263–1299 (1997).
14. S. E. Golowich and M. I. Weinstein, "Scattering resonances and homogenization theory," Bell Labs preprint (Bell Laboratories, Murray Hill, N.J., 2002).
15. A. W. Snyder and J. D. Love, *Optical Waveguide Theory* (Chapman & Hall, London, 1983).
16. P. D. Hislop and I. M. Sigal, *Introduction to Spectral Theory* (Springer-Verlag, New York, 1996).
17. M. Abramowitz and I. E. Stegun, eds., *Handbook of Mathematical Functions* (National Institute of Standards and Technology, Gaithersburg, MD., 1972).
18. The values for the LP_{01} mode calculated by the Fourier expansion were taken from Fig. 3 in Ref. 6.
19. D. Marcuse, *Theory of Dielectric Optical Waveguides*, 2nd ed. (Academic, Boston, 1991).
20. I. S. Gradshteyn and I. M. Ryzhik, *Tables of Integrals, Series and Products* (Academic, New York, 1980).
21. P. Yeh, A. Yariv, and E. Marom, "Theory of Bragg fiber," J. Opt. Soc. Am. **68**, 1196–1201 (1978).